PROCEEDINGS OF SCIENCE

On-the-fly reduction of open loops

Federico Buccioni
University of Zurich, Zurich, SWITZERLAND
E-mail: buccioni@physik.uzh.ch

Jean-Nicolas Lang
University of Zurich, Zurich, SWITZERLAND
E-mail: jlang@physik.uzh.ch

Stefano Pozzorini
University of Zurich, Zurich, SWITZERLAND
E-mail: pozzorin@physik.uzh.ch

Hantian Zhang
University of Zurich, Zurich, SWITZERLAND
E-mail: hantian.zhang@physik.uzh.ch

Max Zoller*
University of Zurich, Zurich, SWITZERLAND
E-mail: zoller@physik.uzh.ch

We describe new developments in the OPENLOOPS framework based on the recently introduced on-the-fly method [1]. The on-the-fly approach exploits the factorisation of one-loop diagrams into segments in order to perform various operations, such as helicity summation, diagram merging and the reduction of Feynman integrands in between the recursion steps for the amplitude construction. This method significantly reduces the complexity of scattering amplitude calculations for multi-particle processes, leading to a major increase in CPU efficiency and numerical stability. The unification of the reduction to scalar integrals with the amplitude construction in a single algorithm, allows to identify problematic kinematical configurations and cure numerical instabilities in single recursion steps. A simple permutation trick in combination with a one-parameter expansion for a single topology, which is now implemented to any order, eliminate rank-two Gram determinant instabilities altogether. Due to this any-order expansion, the numerical accuracy of the algorithm can be determined with a rescaling test. The on-the-fly algorithm is fully implemented for double and quadruple precision, which allows for true quadruple precision benchmarks with up to 32 correct digits as well as a powerful rescue system for unstable points. We present first speed and stability results for these new features. The on-the-fly algorithm is part of the forthcoming release of OPENLOOPS 2.

Loops and Legs in Quantum Field Theory (LL2018)
29 April 2018 - 04 May 2018
St. Goar, Germany

*Speaker.

© Copyright owned by the author(s) under the terms of the Creative Commons Attribution-NonCommercial-NoDerivatives 4.0 International License (CC BY-NC-ND 4.0).

PoS(LL2018)045

1. Automated amplitude generation in OpenLoops

OpenLoops [2, 3] is a fully automated tree-level and one-loop tool for the numerical calculation of high-energy scattering amplitudes, which are a key ingredient in multi-purpose Monte Carlo generators. The helicity- and colour-summed n-particle scattering probability densities

$$\mathscr{W}_{\text{LO}} = \sum_{\text{hel,col}} |\mathscr{M}_0|^2, \quad \mathscr{W}^{\text{virtual}}_{\text{NLO}} = \sum_{\text{hel,col}} 2\,\text{Re}\Big[\mathscr{M}_0^* \mathscr{M}_1\Big] \quad \text{with } \mathscr{M}_l = \sum_d \mathscr{M}_l^{(d)} \tag{1.1}$$

are given by the sums of Feynman diagrams d with $l = 0, 1$ loops and n external particles. A one-loop diagram amplitude can be written as

$$\mathscr{M}_1^{(d)} = \mathscr{C}_1^{(d)} \int \mathrm{d}^D \bar{q}\, \frac{\text{Tr}\Big[\mathscr{N}(q)\Big]}{\bar{D}_0(\bar{q}) \cdots \bar{D}_{N-1}(\bar{q})} = \tag{1.2}$$

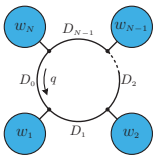

with $\bar{D}_i(\bar{q}) = (\bar{q} + p_i)^2 - m_i^2$ and the colour factor $\mathscr{C}_1^{(d)}$. The loop momentum $\bar{q}$ is a vector in $D = 4 - 2\varepsilon$ dimensions (marked by the bar), whereas the external momenta p_i are four-dimensional. The numerator is constructed by cutting the loop open at one propagator $\bar{D}_0$ and dressing the initial open loop $\mathscr{N}_0 = \mathbb{1}$ in recursion steps

$$\mathscr{N}_n(q) = \mathscr{N}_{n-1}(q) S_k(q), \qquad n \leq N, \tag{1.3}$$

exploiting the factorisation of the numerator into segments,

$$\text{Tr}\Big[\mathscr{N}(q)\Big] = \text{Tr}\Big[\mathscr{N}_N(q)\Big] = \Big[S_1(q)\Big]_{\beta_0}^{\beta_1} \Big[S_2(q)\Big]_{\beta_1}^{\beta_2} \cdots \Big[S_N(q)\Big]_{\beta_{N-1}}^{\beta_N} \delta_{\beta_N}^{\beta_0} = \text{Tr}\Bigg[\tag{1.4}$$

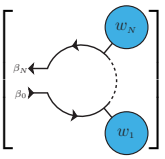

$\Bigg]$.

The Lorentz or spinor indices $\beta_{0,N}$ of the cut propagator are contracted in the last step. A segment consists of a loop vertex and propagator and one or two external subtrees w_i,

$$\Big[S_i(q)\Big]_{\beta_{i-1}}^{\beta_i} = \tag{1.5}$$

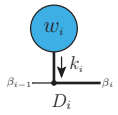

or

$$\Big[S_i(q)\Big]_{\beta_{i-1}}^{\beta_i} = \tag{1.5}$$

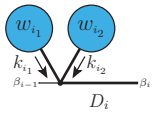

.

Dressing steps are performed numerically for the tensor coefficients $\mathscr{N}^{(n)}_{\mu_1 \ldots \mu_r}$ of the partially constructed open loop,

$$\mathscr{N}_n(q) = \tag{1.6}$$

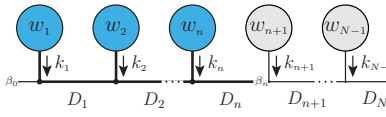

$$= \prod_{i=1}^{k} S_i(q) = \sum_{r=0}^{R} \mathscr{N}^{(n)}_{\mu_1 \ldots \mu_r} q^{\mu_1} \cdots q^{\mu_r}, \tag{1.6}$$

while the analytical structure in the loop momentum and the scalar denominators $\bar{D}_i$ is fully retained. Each dressing step increases the rank R by zero or one in renormalisable models, using

PoS(LL2018)045

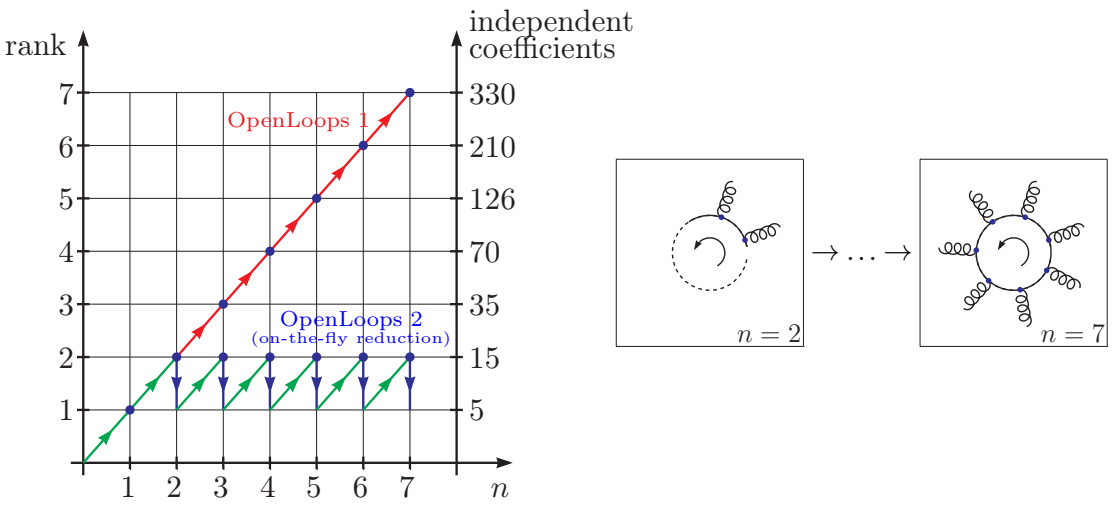

Figure 1: Evolution of the tensor rank and number of independent tensor coefficients in (1.6) with the number n of dressed segments for the example of a seven-gluon scattering amplitude. While in OpenLoops 1 [2] tensor integrals are only reduced after dressing the diagrams, OpenLoops 2 [3] allows for an on-the-fly reduction of tensor integrands. Here a reduction step is performed after the second dressing step, reducing the rank in q to one, before the third dressing step increases the rank again to two. This procedure is continued until the loop is fully dressed.

the Feynman gauge. While in the previous version OpenLoops 1 [2] the tensor reduction was performed a posteriori with external libraries, such as Collier [4] or Cuttools [5], leading to a high tensor rank and number of independent coefficients, the recently introduced on-the-fly reduction [1], implemented in OpenLoops 2 [3], keeps the rank and hence the complexity of intermediate results low (see Fig. 1). In the on-the-fly approach operations such as tensor reduction, diagram merging and partial helicity summations are performed interleaved with the dressing steps (see [1]).

2. The on-the-fly reduction

The on-the-fly reduction formulas are based on [6] and have the form

$$q^\mu q^\nu = \sum_{i=-1}^{3} \left(A_i^{\mu\nu} + B_{i,\lambda}^{\mu\nu} q^\lambda \right) D_i(q) \quad \text{with} \quad D_{-1}(q) = 1, \tag{2.1}$$

where the coefficients $A_i^{\mu\nu}$ and $B_{i,\lambda}^{\mu\nu}$ are q-independent. This is also valid for triangles in renormalisable theories [1,6] if we set terms involving $\bar{D}_3$ and p_3 to zero. The loop momentum dependence resides in the reconstructed denominators $D_i = \bar{D}_i - \tilde{q}^2$ which cancel denominators in the full integrand, leading to four new topologies with pinched propagators. The terms $\propto \tilde{q}^2$, where $\tilde{q} = \bar{q} - q$ is $(D-4)$-dimensional, lead to rational terms of type R_1 [6]. A reduction step (2.1) can be applied to the partial integrand of an open loop, before it reaches rank three, due to the factorised structure of Feynman diagrams,

$$\left[\frac{\mathcal{N}^{\mu\nu} q_\mu q_\nu}{\bar{D}_0 \bar{D}_1 \bar{D}_2 \bar{D}_3} \right] \prod_{i=k+1}^{N} \frac{S_i(q)}{\bar{D}_{i-1}} = \left[\frac{\mathcal{N}_{-1}^{\mu} q_\mu + \mathcal{N}_{-1} + \tilde{\mathcal{N}}_{-1} \tilde{q}^2}{\bar{D}_0 \bar{D}_1 \bar{D}_2 \bar{D}_3} + \sum_{i=0}^{3} \frac{\mathcal{N}_i^{\mu} q_\mu + \mathcal{N}_i}{\bar{D}_0 \cdots \not{\bar{D}}_i \cdots \bar{D}_3} \right] \prod_{i=k+1}^{N} \frac{S_i(q)}{\bar{D}_{i-1}}. \tag{2.2}$$

PoS(LL2018)045

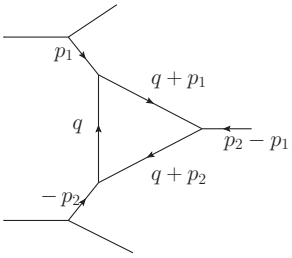

$$\begin{aligned} p_1^2 &= -p^2 < 0, \\ p_2^2 &= -p^2(1+\delta), \qquad 0 \le \delta \ll 1, \\ (p_2-p_1)^2 &= 0 \\ \Rightarrow \sqrt{\Delta} &= \frac{p^2}{2}\delta \end{aligned}$$

Figure 2: Triangle configuration leading to Gram determinant instabilities.

While the complexity due to the tensor rank is kept low throughout the calculation, the creation of pinched topologies potentially leads to a huge proliferation of open loops to be processed. This problem is solved very efficiently by the on-the-fly merging of pinched open loops with open loops of the same topology and the same undressed segments, which can also stem from pinches or correspond to lower-point Feynman diagrams (for details see [1, 7]). The final rank-zero and rank-one tensor integrals are reduced to scalar box, triangle, bubble and tadpole integrals using integral level identities [1, 6], which are then evaluated with COLLIER [4] or ONELOOP [8].

3. Numerical stability and any-order expansions

The main source of numerical instabilities in on-the-fly reduction steps is the appearance of small Gram determinants, especially those constructed from two external momenta,

$$\Delta = -\Delta_{12} = (p_1 \cdot p_2)^2 - p_1^2 p_2^2. \tag{3.1}$$

The three external momenta p_1, p_2, p_3 in the D_i in (2.1) do not play equal roles, since only p_1, p_2 are used in the construction of a basis $l_1, \ldots, l_4$, in which q^μ is decomposed. A simple permutation of the propagators in (2.1),

$$\{D_1, D_2, D_3\} \longrightarrow \{D_{i_1}, D_{i_2}, D_{i_3}\}, \tag{3.2}$$

such that

$$\frac{|\Delta_{i_1 i_2}|}{Q^4_{i_1 i_2}} = \max\left\{\frac{|\Delta_{12}|}{Q^4_{12}}, \frac{|\Delta_{13}|}{Q^4_{13}}, \frac{|\Delta_{23}|}{Q^4_{23}}\right\}, \qquad Q^2_{ij} = \max\{|p_i \cdot p_i|, |p_i^2|, |p_j^2|\} \tag{3.3}$$

allows us to avoid this type of instability completely in topologies with four or more propagators. As a result, a single t-channel topology (Fig. 2) accounts for all rank-two Gram determinant instabilities in the hard phase space region.

In this case, we expand the reduction formula (2.1) (without the $\bar{D}_3$-term) in the small parameter $\delta = \frac{2\sqrt{\Delta}}{-p_1^2}$. Consider for example the rank-one massless-propagator triangle

$$\begin{aligned} C^\mu = \int \mathrm{d}^D q \, \frac{q^\mu}{\bar{D}_0 \bar{D}_1 \bar{D}_2} &= \frac{1}{\delta} C_0\left(p_1^2, p_1^2(1+\delta)\right)\left[-p_1^\mu(1+\delta) + p_2^\mu\right] \\ &+ \frac{2}{\delta^2 p^2}\left\{B_0\left(p_1^2\right)\left[-p_1^\mu(1+\delta) + p_2^\mu\right] + B_0\left(p_1^2(1+\delta)\right)\left[(p_1^\mu - p_2^\mu)(1+\delta)\right]\right\}, \end{aligned} \tag{3.4}$$

PoS(LL2018)045

with

$$C_0(p_1^2,p_2^2) = \int \mathrm{d}^D q \, \frac{1}{\bar{D}_0\bar{D}_1\bar{D}_2}, \qquad B_0(p_1^2) = \int \mathrm{d}^D q \, \frac{1}{\bar{D}_0\bar{D}_1}. \tag{3.5}$$

Separating the reduction formula and the master integral evaluation leads to $\frac{1}{\delta^n}$-poles in intermediate results and hence severe numerical instabilities. If, however, the scalar integrals B_0 and C_0 are expanded in δ directly in (3.4), these poles cancel completely,

$$C^\mu = \frac{p_1^\mu + p_2^\mu}{2p^2}\left[-B_0(p_1^2)+1\right] + \delta\,\frac{p_1^\mu + 2p_2^\mu}{6p^2}\left[B_0(p_1^2)\right] + \mathcal{O}(\delta^2). \tag{3.6}$$

The same behaviour was found for tensor rank up to three in all cases with massless and massive propagators relevant for QCD [1].

A disadvantage of this procedure is that the truncation of the expansion at a fixed order spoils the rescaling test used to estimate the numerical uncertainty of the calculation [1, 2]. In order to avoid this issue we developed and implemented an any-order expansion. Since the $\frac{1}{\delta^n}$-poles in (3.4) cancel, we can substitute

$$\frac{1}{\delta^n} B_0(p_1^2(1+\delta)) \to B_{0,n}(p_1^2,\delta), \qquad \frac{1}{\delta^n} C_0(p_1^2,p_1^2(1+\delta)) \to C_{0,n}(p_1^2,\delta) \tag{3.7}$$

with

$$B_{0,n}(p_1^2,\delta) = \sum_{m=n}^{\infty} \delta^{m-n} \left[\frac{1}{m!}\left(\frac{\partial}{\partial\delta}\right)^m B_0\left(p_1^2(1+\delta)\right)\right]_{\delta=0} \tag{3.8}$$

$$C_{0,n}(p_1^2,\delta) = \sum_{m=n}^{\infty} \delta^{m-n} \left[\frac{1}{m!}\left(\frac{\partial}{\partial\delta}\right)^m C_0\left(p_1^2,p_1^2(1+\delta)\right)\right]_{\delta=0}. \tag{3.9}$$

Our rank-one example (3.4) then takes the form

$$C^\mu = (p_1-p_2)^\mu \left[\frac{B_{0,1}+2B_{0,2}}{p^2} - C_{0,1}\right] + p_1^\mu \left[\frac{B_{0,1}}{p^2} - C_0\right]. \tag{3.10}$$

Closed formulas were derived and implemented for $\left(\frac{\partial}{\partial\delta}\right)^m B_0$ and $\left(\frac{\partial}{\partial\delta}\right)^m C_0$ for all topologies relevant in QCD, and are applied order by order until the relative truncation error becomes smaller than the target precision of 10^{-16} or 10^{-32} in double or quadruple precision calculations respectively. In this way, the truncation error is avoided entirely and the rescaling test of the numerical accuracy is valid. The details of the any-order expansion will be discussed in [9].

In order to illustrate the effect of the various improvements in the on-the-fly reduction of OpenLoops 2, we show the correlation between the instability and the smallest rank-two Gram determinant Δ in a calculation, taking a sample of 10^6 random phase space points for the process $gg \to t\bar{t}gg$. The results without any special treatment of Gram determinants in Fig. 3 (a) show a strong correlation with rank-two Gram determinants over twenty orders of magnitude. In fact, we observe a quadratic or faster scaling in Q_{12}^4/Δ, consistent with the explicit Δ-dependence of the coefficients in (2.1). These results are stabilised using the permutation trick (3.2) and analytic expressions, such as (3.4) for the triangle reduction, as shown in in Fig. 3 (b). Adding fixed-order Gram-determinant expansions, such as (3.6), up to δ^2, introduces a horizontal discontinuity in Fig. 3 (c) due to the threshold, below which the exact formula is replaced by the expansion. Using

PoS(LL2018)045

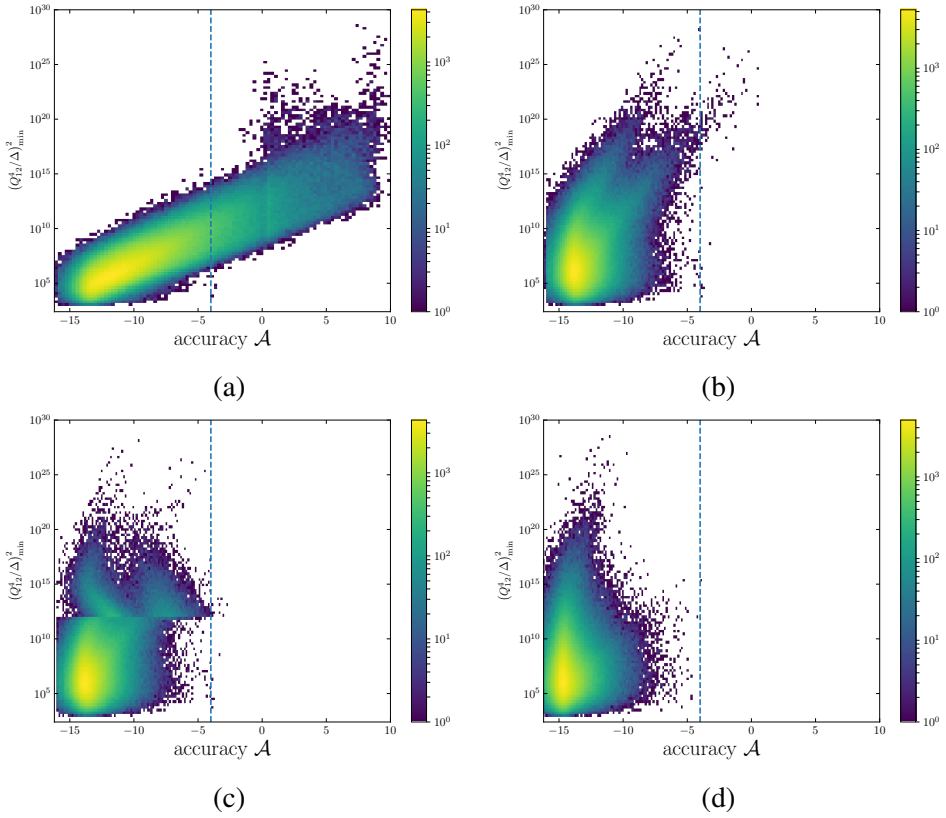

Figure 3: Correlation between the instability $\mathscr{A}$ in double precision and the largest $(Q_{12}^4/\Delta)^2$ in the event, with any rank-two Gram determinant Δ and corresponding Q_{12}^2 from (3.3), in a sample of 10^6 phase space points for $gg \to t\bar{t}gg$. The on-the-fly reduction was used without special treatment of Gram determinants in (a), and with the permutation trick (3.2) and analytic expressions for triangle reduction in (b). In addition to these improvements, the fixed-order Gram-determinant expansions up to δ^2 for $\delta < \delta_{\text{thr}} = 10^{-3}$ were used in (c), and the any-order expansion in (d).

the any-order expansion instead leads to an extremely stable result which does not suffer from a threshold discontinuity as shown in Fig. 3 (d).

We now present numerical stability studies for the on-the-fly algorithm in various modes of OpenLoops. In Fig. 4 we show the fraction of points with an accuracy $\mathscr{A} < \mathscr{A}_{\text{min}}$ plotted against $\mathscr{A}_{\text{min}}$ for a sample of 10^6 homogeneously distributed random phase space points at $\sqrt{s} = 1\,\text{TeV}$, for the process $gg \to t\bar{t}g$. Infrared regions are excluded through cuts, $p_{i,\text{T}} > 50\,\text{GeV}$ and $\Delta R_{ij} > 0.5$ for massless final-state partons.

The numerical accuracy of the double precision (dp) results is defined w.r.t. a quadruple precision (qp) benchmark, $\mathscr{A} = \log_{10}|(\mathscr{W}_{\text{dp}} - \mathscr{W}_{\text{qp}})/\min\{|\mathscr{W}_{\text{dp}}|, |\mathscr{W}_{\text{qp}}|\}|$. The qp benchmark is derived in OpenLoops 2 with the on-the-fly reduction (OL2), which is fully implemented in dp and qp, including all stability improvements. The final scalar integrals are evaluated with OneLoop 3.6.1 [8] in qp. The accuracy of the benchmark OL2_qp is determined with the rescaling test. This is the first full qp implementation of a one-loop amplitude generator, yielding up to 32 correct digits. For this process only one out of a million phase space points has less than 20 correct digits. This is in

PoS(LL2018)045

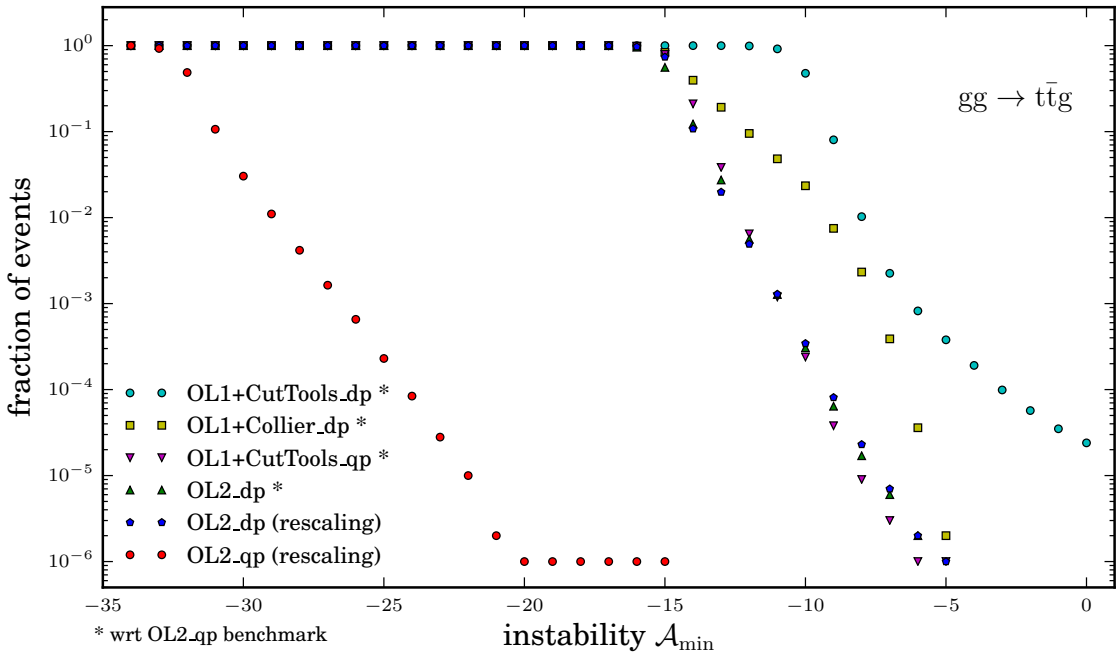

Figure 4: Stability distributions for a sample $2 \to 3$ process.

contrast to OpenLoops 1 (OL1) with Cuttools 1.9.5 [5] in qp, where dp-contamination inside Cuttools prevents more than 16 correct digits. The scalar integrals for OL2 calculations in dp were evaluated with Collier 1.2 [4].

For this process, OL2 in dp yields an improvement of $1-3$ orders of magnitude in numerical accuracy as compared to OL1+Collier in dp, which in turn gains many orders of magnitude compared to OL1+Cuttools in dp, especially in the tail, where the latter becomes unreliable. In fact, the accuracy of OL2 in dp is comparable to OL1+Cuttools in qp, which used to be the benchmark in OpenLoops 1. The accuracy of OL2 was measured once against the OL2_qp benchmark and once with the rescaling test, the results of which are in excellent agreement. In OpenLoops 2 we use a stability rescue system for dp calculations similar to the one in OpenLoops 1, which is based on the rescaling test in dp and a re-run in qp for phase space points, for which a target accuracy is not reached.

4. CPU efficiency

In this section we briefly discuss the speed of the on-the-fly algorithm. The upper frame in Fig. 5 shows the runtime versus the number of one-loop Feynman diagrams for four $2 \to 2+n$ process classes with $n = 0,\ldots,3$ additional gluons in the final state. We find in good approximation, that the order of magnitude of the runtime scales linearly with the order of magnitude of the number of one-loop diagrams. Computing a phase space point in qp takes a factor $20-80$ longer than in dp, depending on the process. In high-multiplicity processes, this factor tends to be larger than in simple $2 \to 2$ processes. The lower frame shows the ratio between the OL2 runtime in qp to the OL1+Cuttools runtime in qp, where we find a gain in speed of a factor $3-5$ due to the on-the-fly

PoS(LL2018)045

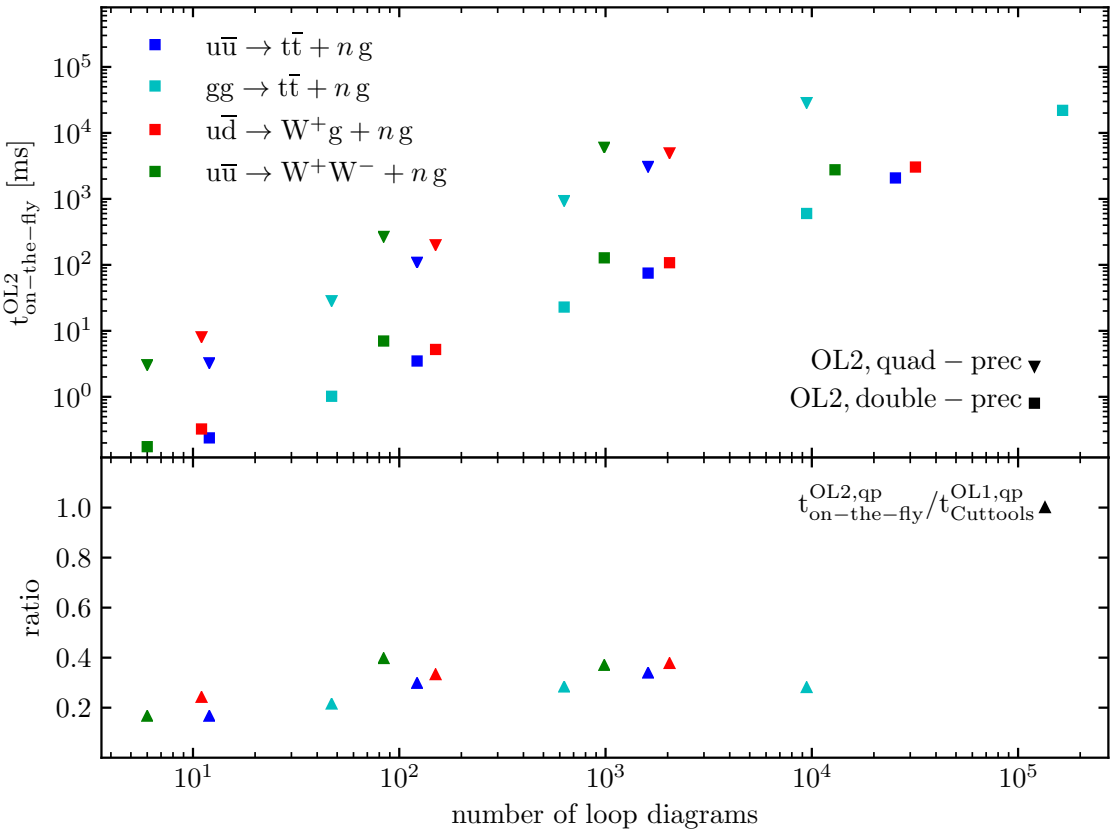

Figure 5: CPU runtimes per phase space point on a single Intel i7-4790K core with gfortran-4.8.5 for a one-loop scattering probability density plotted versus the number of one-loop diagrams in double (dp) and quadruple precision (qp). From left to right, the number of additional gluons is $n = 0,\ldots,3$ in dp and $n = 0,\ldots,2$ in qp. In the lower frame the ratio of the runtime in OpenLoops 2 (OL2) in qp to the runtime in OpenLoops 1+Cuttools (OL1) in qp is presented.

method. Hence, the efficiency improvement in OpenLoops due to the on-the-fly method is even more pronounced in qp than in dp, where we found a speed-up of a factor $2-3$ [1].

5. Conclusion

We have presented the on-the-fly method for the automated calculation of scattering amplitudes at one loop. Exploiting the factorised structure of open loops in a systematic way, we perform operations, such as tensor reduction, helicity summation and diagram merging, on-the-fly during the open-loop recursion. This approach reduces the complexity of intermediate results and operations significantly, leading to a substantial gain in CPU efficiency.

The on-the-fly integrand reduction allows us to isolate Gram determinant instabilities in triangle topologies with a particular kinematic configuration and to cure them by means of simple analytic expansions, which can be performed to any order. With a small set of simple optimisations the on-the-fly algorithm achieves an unprecedented level of numerical stability, which is a particularly attractive feature for the calculation of real–virtual contributions at NNLO.

PoS(LL2018)045

This algorithm is fully implemented in double and quadruple precision, and validated for a wide range of SM processes at NLO QCD. It will become publicly available in the upcoming release of OPENLOOPS 2.

Acknowledgements

This research was supported in part by the Swiss National Science Foundation (SNF) under contracts PP00P2-128552 and BSCGI0-157722.

References

[1] F. Buccioni, S. Pozzorini and M. Zoller, *On-the-fly reduction of open loops*, *Eur. Phys. J.* **C78** (2018) 70, [1710.11452].

[2] F. Cascioli, P. Maierhöfer and S. Pozzorini, *Scattering Amplitudes with Open Loops*, *Phys.Rev.Lett.* **108** (2012) 111601, [1111.5206].

[3] F. Buccioni, J. Lindert, P. Maierhofer, S. Pozzorini and M. Zoller, *OpenLoops 2*, *in preparation*.

[4] A. Denner, S. Dittmaier and L. Hofer, *Collier: a fortran-based Complex One-Loop LIbrary in Extended Regularizations*, *Comput. Phys. Commun.* **212** (2017) 220–238, [1604.06792].

[5] G. Ossola, C. G. Papadopoulos and R. Pittau, *CutTools: A Program implementing the OPP reduction method to compute one-loop amplitudes*, *JHEP* **03** (2008) 042, [0711.3596].

[6] F. del Aguila and R. Pittau, *Recursive numerical calculus of one-loop tensor integrals*, *JHEP* **07** (2004) 017, [hep-ph/0404120].

[7] F. Buccioni, S. Pozzorini and M. Zoller, *A new method for one-loop amplitude generation and reduction in OpenLoops*, *PoS* **RADCOR2017** (2017) 024, [1801.03772].

[8] A. van Hameren, *OneLoop: For the evaluation of one-loop scalar functions*, *Comput.Phys.Commun.* **182** (2011) 2427–2438, [1007.4716].

[9] F. Buccioni, J.-N. Lang, S. Pozzorini, H. Zhang and M. Zoller, *Numerical stability of the on-the-fly method in OpenLoops 2*, *in preparation*.

PoS(LL2018)045